A Crystallographic Map of Chiral Recognition in π Complexes of Aromatic Aldehydes and a Chiral Transition Metal Lewis Acid: Enantioface Binding Selectivities in Solution Correlate to Distances between Metal and Carbon Stereocenters in the Solid State

Brian J. Boone, Darryl P. Klein, Jeffery W. Seyler, N. Quirós Méndez, A. M. Arif, and J. A. Gladysz*

Contribution from the Department of Chemistry, University of Utah, Salt Lake City, Utah 84112

Received October 20, 1995[⊗]

Abstract: The π aromatic aldehyde complexes $[(\eta^5\text{-}C_5H_5)Re(NO)(PPh_3)(\eta^2\text{-}O{=}CHAr)]^+BF_4^-$ (**1**$^+BF_4^-$; Ar = **a**, C_6F_5; **b**, 4-$C_6H_4CF_3$; **c**, 4-C_6H_4Cl; **d**, C_6H_5; **e**, 4-$C_6H_4CH_3$; **f**, 4-$C_6H_4CH_2CH_3$; **g**, 4-$C_6H_4OCH_3$) exist as mixtures of configurational diastereomers (*RS*,*SR*/*RR*,*SS* or π/π') that differ in the O═C enantioface bound to rhenium. Under standard conditions (0.000 71 M, CH_2Cl_2, 173 K), π/π' equilibrium ratios are 97:3, 89:11, 84:16, 80:20, 76:24, 79:21, and 74:26, respectively. Steric interactions between the aryl groups and cyclopentadienyl ligands destabilize the π' isomers. The crystal structures of (*RS*,*SR*)-**1a**−**c**,**f**$^+PF_6^-$ and (*RS*,*SR*)-**1d**$^+SbF_6^-$ show that the distances between the rhenium and carbon stereocenters (Å, **a**/**b**/**c**/**d**/**f**: 2.157(5)−2.161(9), 2.172(4), 2.176(4), 2.182(6)−2.188(9), 2.184-(5)−2.199(6)) increase as π/π' ratios decrease. Stronger π accepting aldehydes give shorter bonds and higher chiral recognition. The aliphatic aldehyde complexes $[(\eta^5\text{-}C_5H_5)Re(NO)(PPh_3)(\eta^2\text{-}O{=}CHR)]^+BF_4^-$ exhibit higher π/π' ratios (R = CH_3, 99.0:1.0; CH_2CH_3, 99.8:0.2; $CH_2CH_2CH_3$, 99.5:0.5; $CH(CH_3)_2$ and $C(CH_3)_3$, >99.9:<0.1), and possible rationales are given. The π/π' ratios increase at higher concentration or lower temperature, and vary slightly with counteranion ($BF_4^- > PF_6^- \geq SbF_6^-$).

Most types of bonding interactions between two chiral or prochiral species offer the potential for "chiral recognition"—the selective formation of one of two possible diastereomeric adducts.[1] Such phenomena play critical roles in numerous biological processes and two extremely active areas of chemical research: enantiomer separations via "chiral chromatography" [2] and enantioselective organic syntheses.[3]

Steric effects are of obvious importance in chiral recognition and have been well documented. Surprisingly, there have been very few investigations of electronic effects.[1a] The variation of electronic properties of binding partners could provide a valuable means of optimizing selectivity. Recently, fascinating electronic effects in transition metal-mediated asymmetric catalysis have been reported.[4,5] However, in most cases the mechanistic basis for the trends observed remains poorly understood. Hence, we set out to probe for electronic effects in chiral recognition phenomena involving metal π complexes, which are intermediates in diverse types of enantioselective reactions.[3]

Over the last decade, we have undertaken extensive studies of complexes of the chiral rhenium Lewis acid $[(\eta^5\text{-}C_5H_5)Re(NO)(PPh_3)]^+$ (**I**) with organic and inorganic Lewis bases.[6−11] This 16-valence-electron fragment is a strong π donor, with the d orbital HOMO shown in Chart 1.[12] Hence, unsaturated ligands

⊗ Abstract published in *Advance ACS Abstracts,* February 15, 1996.

(1) Lead references to an extensive literature: (a) Peacock, S. C.; Domeier, L. A.; Gaeta, F. C. A.; Helgeson, R. C.; Timko, J. M.; Cram, D. J. *J. Am. Chem. Soc*. **1978**, *100*, 8190. (b) Peacock, S. S.; Walba, D. M.; Gaeta, F. C. A.; Helgeson, R. C.; Cram, D. J. *J. Am. Chem. Soc*. **1980**, *102*, 2043. (c) Galán, A.; Andreu, D.; Echavarren, A. M.; Prados, P.; de Mendoza, J. *J. Am. Chem. Soc*. **1992**, *114*, 1511. (d) Andelman, D.; Orland, H. *J. Am. Chem. Soc*. **1993**, *115*, 12322. (e) Owens, L.; Thilgen, C.; Diederich, F.; Knobler, C. B. *Helv. Chim. Acta* **1993**, *76*, 2757, and references therein. (f) Burger, M. T.; Armstrong, A.; Guarnieri, F.; McDonald, D. Q.; Still, W. C. *J. Am. Chem. Soc*. **1994**, *116*, 3593. (g) Mizutani, T.; Ema, T.; Tomita, T.; Kuroda, Y.; Ogoshi, H. *J. Am. Chem. Soc*. **1994**, *116*, 4240. (h) Sawada, M.; Takai, Y.; Yamada, H.; Hirayama, S.; Kaneda, T.; Tanaka, T.; Kamada, K.; Mizooku, T.; Takeuchi, S.; Ueno, K.; Hirose, K.; Tobe, Y.; Naemura, K. *J. Am. Chem. Soc*. **1995**, *117*, 7726.

(2) (a) Schurig, V.; Nowotny, H.-P. *Angew. Chem., Int. Ed. Engl*. **1990**, *29*, 939, and references therein. (b) *Chiral Liquid Chromatography*; Lough, W. J. Ed.; Chapman and Hall: New York, 1989. (c) *Chiral Separations by Liquid Chromatography*; Ahuja, S., Ed.; American Chemical Society (Symposium Series #471): Washington DC, 1991. (d) Camilleri, P.; Eggleston, D. S.; Rzepa, H. S.; Webb, M. L. *J. Chem. Soc., Chem. Commun*. **1994**, 1135.

(3) *Catalytic Asymmetric Synthesis*; Ojima, I. Ed.; VCH: New York, 1993.

(4) (a) Chang, S.; Heid, R. M.; Jacobsen, E. N. *Tetrahedron Lett*. **1994**, *35*, 669, and earlier papers cited therein. (b) RajanBabu, T. V.; Casalnuovo, A. L. *Pure Appl. Chem*. **1994**, *66*, 1535. (c) Hawkins, J. M.; Loren, S.; Nambu, M. *J. Am. Chem. Soc*. **1994**, *116*, 1657. (d) Schnyder, A.; Hintermann, L.; Togni, A. *Angew. Chem., Int. Ed. Engl*. **1995**, *34*, 931, and references therein.

(5) See also Halterman, R. L.; McEvoy, M. A. *J. Am. Chem. Soc*. **1992**, *114*, 980.

(6) Aliphatic aldehyde complexes of **I**: (a) Garner, C. M.; Quirós Méndez, N.; Kowalczyk, J. J.; Fernández, J. M.; Emerson, K.; Larsen, R. D.; Gladysz, J. A. *J. Am. Chem. Soc*. **1990**, *112*, 5146. (b) Dalton, D. M.; Garner, C. M.; Fernández, J. M.; Gladysz, J. A. *J. Org. Chem*. **1991**, *56*, 6823. (c) Klein, D. P.; Quirós Méndez, N.; Seyler, J. W.; Arif, A. M.; Gladysz, J. A. *J. Organomet. Chem*. **1993**, *450*, 157.

(7) Aromatic aldehyde complexes of **I**: (a) Quirós Méndez, N.; Arif, A. M.; Gladysz, J. A. *Angew. Chem., Int. Ed. Engl*. **1990**, *29*, 1473. (b) Quirós Méndez, N.; Mayne, C. L.; Gladysz, J. A. *Angew. Chem., Int. Ed. Engl*. **1990**, *29*, 1475. (c) Klein, D. P.; Gladysz, J. A. *J. Am. Chem. Soc*. **1992**, *144*, 8710. (d) Quirós Méndez, N.; Seyler, J. W.; Arif, A. M.; Gladysz, J. A. *J. Am. Chem. Soc*. **1993**, *115*, 2323. (e) Boone, B. J.; Klein, D. P.; Quirós Méndez, N.; Seyler, J. W.; Arif, A. M.; Gladysz, J. A. *J. Chem. Soc., Chem. Commun*. **1995**, 279.

(8) Monosubstituted alkene complexes of **I**: (a) Bodner, G. S.; Peng, T.-S.; Arif, A. M.; Gladysz, J. A. *Organometallics* **1990**, *9*, 1191. (b) Peng, T.-S.; Arif, A. M.; Gladysz, J. A. *Helv. Chim. Acta* **1992**, *75*, 442. (c) Peng, T.-S.; Gladysz, J. A. *J. Am. Chem. Soc*. **1992**, *114*, 4174. (d) Peng, T.-S.; Gladysz, J. A. *Organometallics* **1995**, *14*, 898. (e) Wang, Y.; Gladysz, J. A. *Chem. Ber*. **1995**, *128*, 213. (f) Peng, T.-S.; Arif, A. M.; Gladysz, J. A. *J. Chem. Soc., Dalton Trans*. **1995**, 1857. (g) Sanau, M.; Peng, T.-S.; Arif, A. M.; Gladysz, J. A. *J. Organomet. Chem*. **1995**, *503*, 235.

0002-7863/96/1518-2411$12.00/0

Chart 1. **I**: d-Orbital HOMO of the Pyramidal Rhenium Fragment $[(\eta^5\text{-}C_5H_5)Re(NO)(PPh_3)]^+$; **II** and **III**: Idealized Structures of Diastereomeric Aldehyde and Monosubstituted Alkene Complexes of **I**

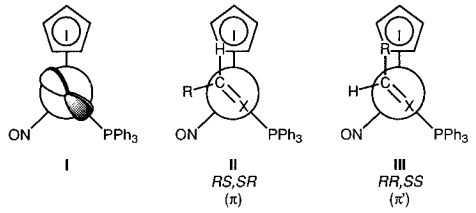

commonly adopt conformations that allow high degrees of overlap with their acceptor orbitals. This electronic feature, together with steric properties of the other rhenium ligands, can lead to high degrees of chiral recognition.[6−11]

For example, **I** forms π complexes with aliphatic aldehydes and monosubstituted alkenes (X═CHR). There are two conformations about the Re-(X═CHR) axes that maximize overlap of the HOMO of **I** and X═C π^* acceptor orbitals. That in which the larger ═CHR terminus is *anti* to the bulky PPh_3 ligand is greatly favored sterically. Within this constraint, two configurational diastereomers remain possible, as depicted by **II** (*RS*,*SR* or π) and **III** (*RR*,*SS* or π') in Chart 1.[13,14] These differ in the positions of the alkyl and hydrogen substituents or, equivalently, the X═C enantioface bound to rhenium. Diastereomer **II**, in which the alkyl group is directed away from the larger cyclopentadienyl ligand and *syn* to the small nitrosyl ligand, is greatly favored sterically. Thus, very high levels of chiral recognition or thermodynamic enantioface binding selectivities are observed.[6a,8c]

We wondered whether electronic effects upon enantioface binding selectivities were possible in such compounds. However, the **II**/**III** or π/π' ratios were generally too high to easily measure statistically meaningful differences. We then prepared a series of *aromatic* aldehyde complexes $[(\eta^5\text{-}C_5H_5)Re(NO)(PPh_3)(O{=}CHAr)]^+X^-$ (**1**$^+X^-$), which as illustrated in Scheme 1 were usually mixtures of π/π' (**IV**/**V**) and σ isomers in solution.[7] As detailed in a preceding full paper,[7d] $(\pi+\pi')/\sigma$ equilibrium ratios were sensitive functions of the aryl substituents. Electron withdrawing groups, which enhance aldehyde π acidity and diminish σ basicity, favored the π/π' binding modes. Conversely, electron donating groups favored the σ binding mode. Furthermore, the π/π' equilibrium ratios now spanned a relatively large range and were *much higher* with electron withdrawing aryl substituents.[7b]

Scheme 1. Summary of Aldehyde Complexes Studied and Previously Reported π/σ Equilibria

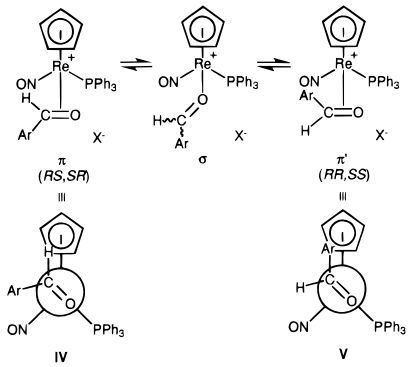

Cmpd	Ar	$(\pi+\pi')/\sigma$, CH_2Cl_2, 299 K
1a$^+$ BF_4^-	C_6F_5	>96:<4
1b$^+$ BF_4^-	4-$C_6H_4CF_3$	>96:<4
1c$^+$ BF_4^-	4-C_6H_4Cl	83:17
1d$^+$ BF_4^-	C_6H_5	84:16
1e$^+$ BF_4^-	4-$C_6H_4CH_3$	53:47
1f$^+$ BF_4^-	4-$C_6H_4CH_2CH_3$	50:50
1g$^+$ BF_4^-	4-$C_6H_4OCH_3$	15:85

We thought, perhaps optimistically, that the trend in π/π' ratios might reduce to a simple one-parameter explanation. Namely, *distances between the rhenium and carbon stereocenters should decrease in complexes of the more* π *acidic aldehydes*. This can be viewed as an electronic effect upon bond length and would in turn enhance steric interactions between the cyclopentadienyl ligand and O═CH***Ar*** substituents in the π' isomers, giving higher π/π' ratios and chiral recognition.[15] In this event, correlations to crystallographic rhenium−carbon bond lengths would be expected.

In this paper, we report a detailed study of chiral recognition in π complexes of **I** and seven representative aromatic aldehydes: **a**, pentafluorobenzaldehyde; **b**, *p*-trifluoromethylbenzaldehyde; **c**, *p*-chlorobenzaldehyde; **d**, benzaldehyde; **e**, *p*-methylbenzaldehyde; **f**, *p*-ethylbenzaldehyde; **g**, *p*-methoxybenzaldehyde (**1a**−**g**$^+X^-$; Scheme 1). The crystal structures of five compounds are determined at room or low temperature and support the controlling basis proposed above for the π/π' ratio trend. For comparison, related data are also given for the π aliphatic aldehyde complexes $[(\eta^5\text{-}C_5H_5)Re(NO)(PPh_3)(\eta^2\text{-}O{=}CHR)]^+X^-$ (**2**$^+X^-$).[6] A portion of this work has been communicated.[7a,e] The mechanism of interconversion of π/π' isomers—a rapid nondissociative process involving σ isomers as sketched in Scheme 1—will be detailed in a separate publication.[7b,16]

Results

1. Configurational Diastereomers of Aromatic Aldehyde Complexes. Variable temperature $^{31}P\{^1H\}$, ^1H, and $^{13}C\{^1H\}$ NMR spectra of **1a**−**g**$^+BF_4^-$ were recorded in CD_2Cl_2.[17] At sufficiently low temperatures, most resonances decoalesced to those of π and π' isomers (**IV** and **V**, Scheme 1). Samples froze near 173 K. Representative spectra are depicted in Figure 1, selected chemical shift data are given in Table 1,[18] and π/π' ratios are summarized below. The ^{31}P and cyclopentadienyl ^{13}C resonances of the π isomers (8.9−9.3, 98.2−99.5 ppm) were upfield of those of the π' isomers (11.0−11.9, 100.8−102.0

(9) 1,3-Enone, enal, diene, and glyoxal complexes of **I**: (a) Wang, Y.; Agbossou, F.; Dalton, D. M.; Liu, Y.; Arif, A. M.; Gladysz, J. A. *Organometallics* **1993**, *12*, 2699. (b) Peng, T.-S.; Wang, Y.; Arif, A. M.; Gladysz, J. A. *Organometallics* **1993**, *12*, 4535. (c) Wang, Y.; Arif, A. M.; Gladysz, J. A. *Organometallics* **1994**, *13*, 2164.

(10) Other alkene complexes of **I**: (a) Kowalczyk, J. J.; Arif, A. M.; Gladysz, J. A. *Chem. Ber.* **1991**, *124*, 729. (b) Pu, J.; Peng, T.-S.; Mayne, C. L.; Arif, A. M.; Gladysz, J. A. *Organometallics* **1993**, *12*, 2686. (c) Peng, T.-S.; Pu, J.; Gladysz, J. A. *Organometallics* **1994**, *13*, 929.

(11) Analogous *pentamethyl*cyclopentadienyl aldehyde and alkene complexes: (a) Agbossou, F.; Ramsden, J. A.; Huang, Y.-H.; Arif, A. M.; Gladysz, J. A. *Organometallics* **1992**, *11*, 693. (b) Peng, T.-S.; Winter, C. H.; Gladysz, J. A. *Inorg. Chem.* **1994**, *33*, 2534.

(12) (a) Schilling, B. E. R.; Hoffmann, R.; Faller, J. W. *J. Am. Chem. Soc.* **1979**, *101*, 592. (b) Czech, P. T.; Gladysz, J. A.; Fenske, R. F. *Organometallics* **1989**, *8*, 1806.

(13) (a) The absolute configuration of the rhenium stereocenter is specified prior to that of carbon stereocenter, following conventions described previously.[6a,10b] Carbon configurations are omitted for mixtures of enantiomerically pure π/π' isomers. (b) All isomer ratios are normalized to 100.

(14) Two Re-(C═C) rotamers can be detected for some alkene complexes of **I**.[8e,9a,10c] The ═*CH* ^1H and ^{13}C NMR resonances of the C═C terminus *syn* to the PPh_3 ligand always show significant phosphorus coupling, whereas those of the C═C terminus *anti* to the PPh_3 ligand do not.

(15) The rhenium−carbon bond lengths in **1**$^+X^-$ would not necessarily be equal in π and π' isomers. However, they should undergo parallel changes as aryl substituents are varied.

(16) Boone, B. J.; Quirós Méndez, N.; Mayne, C. L.; Gladysz, J. A. manuscript in preparation.

(17) Complex **1f**$^+BF_4^-$ has not been reported previously. It was prepared and characterized similarly to the other complexes (Experimental Section).

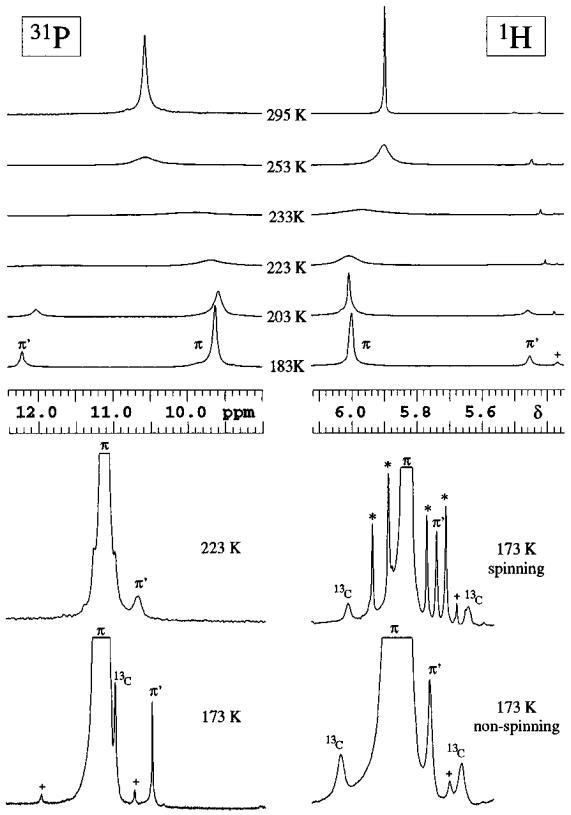

Figure 1. Representative variable temperature NMR spectra: (top) $^{31}P\{^1H\}$ and ^1H spectra of benzaldehyde complex **1d**$^+BF_4^-$ and (bottom) $^{31}P\{^1H\}$ and spinning and nonspinning ^1H spectra of acetaldehyde complex **2a**$^+BF_4^-$ (+ = impurity, * = spinning sideband, ^{13}C = ^{13}C satellite).

ppm). However, the cyclopentadienyl ^1H resonances of the π' isomers (δ 5.44−5.82) were upfield of those of the π isomers (δ 5.94−6.21). The latter shielding trend follows logically from the position of the O═C aryl substituent in **V**. Only in the case of *p*-methoxybenzaldehyde complex **1g**$^+BF_4^-$ was a σ isomer detected (22.4 ppm; $\pi/\pi'/\sigma$ 33:11:56, 173 K). The $(\pi+\pi')/\sigma$ ratios in Scheme 1 have previously been shown to dramatically increase at low temperatures.[7d]

The assignment of the resonances in Figure 1 and Table 1 to π/π' isomers, as opposed to other possibilities, was justified as follows. First, styrene can be considered roughly isosteric with benzaldehyde. The π/π' isomers of the styrene complex $[(\eta^5\text{-}C_5H_5)Re(NO)(PPh_3)(H_2C{=}CHC_6H_5)]^+BF_4^-$ do not rapidly interconvert at room temperature and have been independently isolated[8a−c] and crystallographically characterized.[8g] Their NMR chemical shift trends parallel those in Table 1 (π/π': ^{31}P 10.5/10.7 ppm; ^1H δ 5.77/5.22; ^{13}C 97.5/99.9 ppm). Furthermore, equilibration (chlorohydrocarbon solvents, 368−373 K) gives a comparable π/π' ratio (90:10). Finally, conformers that differ by 180° rotations about the Re-(O═C) axes in **IV** or **V** should give O═*CH* ^1H and ^{13}C resonances that are coupled to phosphorus.[14] None of the resonances in Table 1 exhibited resolved phosphorus couplings.

Since $\Delta G^{\neq}$ values for the interconversion of π and π' isomers are easily calculated from the preceding data, they are presented in Table 1 at this time. As communicated earlier,[7b] they decrease as the free energy differences between π and σ isomers decrease. However, these values will be more fully interpreted in a future paper on the dynamic properties of these compounds.[16] It should be emphasized that they are derived from samples under "nonstandard" conditions (see below) and differ slightly from those given earlier due to the application of a less approximate formula.[19]

2. Binding Selectivities of Aromatic Aldehydes. Standard Conditions. For the purpose of the correlation sought in the introduction, accurate π/π' equilibrium ratios were needed. Some values were given in two earlier reports.[7b,c] However, as more and more data were compiled, variations were noted. Ultimately, unanticipated concentration and counteranion dependences were discovered as outlined below. Thus, all π/π' ratios were determined by ^{31}P NMR under a set of "standard conditions" (0.000 71 M,[20] CH_2Cl_2) at 183 and 173 K as summarized in Table 2. Due to the low decoalescence temperature of *p*-methoxybenzaldehyde complex **1g**$^+BF_4^-$, data were acquired only at 173 K.

The standard conditions were necessarily dilute in order to accommodate the least soluble compound (**1d**$^+X^-$). This in turn required relatively long acquisition times, especially to achieve adequate signal/noise (S/N) for the less intense π' resonances. For each complex, at least four independently prepared samples were assayed. Raw data are summarized in the supporting information. Importantly, measurements of peak integrals, heights, and masses gave identical results. Standard deviations are given in the footnotes of Table 2 and establish error limits ranging from 0.3 to 1.7 on each integer of the normalized isomer ratios.[13b,21]

3. Aromatic Aldehyde Binding Selectivities as Functions of Concentration, Counteranion, Configuration, and Temperature. The concentrations of CH_2Cl_2 solutions of *p*-methylbenzaldehyde complex **1e**$^+BF_4^-$ were varied over a >200-fold range from 0.000 709 M to 0.156 M.[20] As summarized in Table 3, π/π' equilibrium ratios increased monotonically from 73:27 (^{31}P NMR: 11.7/9.3 ppm) to 83:17 (12.1/9.7 ppm) at 183 K and from 76:24 (11.8/9.3 ppm) to 85:15 (12.2/9.7 ppm) at 173 K. Hence, binding selectivities are greater at higher concentrations.

Hexafluorophosphate and hexafluoroantimonate analogs of **1a**−**g**$^+BF_4^-$ can be prepared by simple metathesis procedures. Thus, the π/π' equilibrium ratios of benzaldehyde complexes **1d**$^+BF_4^-$, **1d**$^+PF_6^-$, and **1d**$^+SbF_6^-$ were measured under the standard conditions. The binding selectivities decreased slightly, as summarized in Table 4 (78:22, 74:26, 73:27 at 183 K; ^{31}P NMR: 11.7/9.8, 11.7/9.8, 11.5/9.8 ppm). Parallel trends were observed with the *p*-chlorobenzaldehyde and *p*-methylbenzaldehyde complexes **1c**,**e**$^+BF_4^-$ and **1c**,**e**$^+PF_6^-$. The enantiomerically pure benzaldehyde complex[6a,13a] (+)-(*R*)-**1d**$^+BF_4^-$ gave π/π' ratios identical with those of the racemate. This much more soluble compound also exhibited higher π/π' ratios at higher concentrations (Table 4).

The data at 183 and 173 K in Tables 2−4 suggested that the π/π' equilibrium ratios were temperature dependent. Thus, ^{31}P spectra of a 0.0074 M CH_2Cl_2 solution (ca. ten times the

(18) At 183 K, **1b**,**c**$^+BF_4^-$ (but not **1d**,**e**$^+BF_4^-$) also exhibited two O═CH ^1H resonances (π/π' δ 6.42/6.32, 6.45/6.37), and **1e**$^+BF_4^-$ gave two methyl ^1H resonances (π/π' δ 2.54/2.39). Similarly, **1d**,**e**$^+BF_4^-$ (but not **1a**,**b**,**c**$^+BF_4^-$) showed two O═CH ^{13}C resonances (π/π', 75 MHz: 75.2/74.8, 76.0/75.8 ppm; baseline resolved at 125 MHz).

(19) Sandström, J. *Dynamic NMR Spectroscopy*; Academic Press: New York, 1982. Coalescence temperatures were determined graphically from line widths (pp 81−84), and $\Delta G^{\neq}$ calculations utilized equation 6.5c, as opposed to 6.7a.

(20) (a) For uniformity, all sample concentrations are given at 293 K. The density of CH_2Cl_2 varies from 1.325 g/mL at 293 K to 1.508 g/mL at 193 K: *Industrial Solvents Handbook*, 4th ed.; Flick, E. W., Ed.; Noyes Data Corp: Park Ridge, NJ, 1991. (b) The data in Table 3 show that the concentration of **1e**$^+BF_4^-$ must be more than doubled to effect binding selectivity increases comparable to those observed when samples are cooled by 10−20 K (Table 5). Since the density of CH_2Cl_2 varies only slightly over these intervals, concentration effects play only minor roles in temperature dependences.

(21) For a discussion of error limits on integrals in nonreplicated NMR spectra, see: Derome, A. E. *Modern NMR Techniques for Chemistry Research*; Pergamon: New York, 1987; Chapter 7.6.

Table 1. NMR, T_c, and $\Delta G^{\ddagger}$ Data for Diastereomeric π Aromatic Aldehyde Complexes [(η^5-C_5H_5)Re(NO)(PPh_3)(η^2-O=CHAr)]$^+BF_4^-$ (**1**$^+BF_4^-$)

		NMR (π/π'; 183 K, CD_2Cl_2)				
compd	Ar	$^{31}P\{^1H\}$ (ppm)	^1H (δ, C_5H_5)	$^{13}C\{^1H\}$ (ppm, C_5H_5)	T_c (K) ($^{31}P/^1H/^{13}C$)	$\Delta G^{\ddagger}$ (kcal/mol)[a] ($^{31}P/^1H/^{13}C$)
1a$^+BF_4^-$	C_6F_5	9.3/11.0	6.21/5.82	99.4/101.1	>300/>300/>300	>16.2/>16.6/>16.5
1b$^+BF_4^-$	4-$C_6H_4CF_3$	9.1/11.7	6.18/5.61	98.7/101.1	278/274/274	13.9/14.0/14.0
1c$^+BF_4^-$	4-C_6H_4Cl	8.9/11.6	6.14/5.61	99.5/101.9	246/241/241	12.0/12.1/12.1
1d$^+BF_4^-$	C_6H_5	9.1/11.7	6.10/5.55	99.5/102.0	234/231/232	11.4/11.5/11.5
1e$^+BF_4^-$	4-$C_6H_4CH_3$	9.3/11.7	6.08/5.54	98.4/100.9	212/214/213	10.2/10.6/10.4
1f$^+BF_4^-$	4-$C_6H_4CH_2CH_3$	9.3/11.8	5.99/5.44	98.2/100.8	214/213/−	10.2/10.4/−
1g$^+BF_4^-$	4-$C_6H_4OCH_3$	9.3/11.9[b]	5.94/5.69[b]		186/177/−	8.5/8.6/−

[a] For conversion of the π (*RS*,*SR*) isomer to the π' (*RR*,*SS*) isomer and from π/π' ratios (183 K unless noted) of **a**, 98:2 (0.062 M); **b**, 91:9 (0.13 M); **c**, 87:13 (0.032 M); **d**, 85:15 ((+)-(*R*)-**1d**$^+BF_4^-$, 0.076 M); **e**, 82:18 (0.14 M); **f**, 79:21 (0.021 M); **g**, 74:26 (173 K, 0.00071 M). [b] These data were recorded at 173 K on a 500 MHz spectrometer. Other data were recorded on a 300 MHz spectrometer.

Table 2. Summary of Aromatic Aldehyde Binding Selectivities under "Standard Conditions" [a]

		π/π' [b]	
compd	Ar	183 K	173 K
1a$^+BF_4^-$	C_6F_5	97:3	97:3
1b$^+BF_4^-$	4-$C_6H_4CF_3$	88:12	89:11
1c$^+BF_4^-$	4-C_6H_4Cl	83:17	84:16
1d$^+BF_4^-$	C_6H_5	78:22	80:20
1e$^+BF_4^-$	4-$C_6H_4CH_3$	73:27	76:24
1f$^+BF_4^-$	4-$C_6H_4CH_2CH_3$	75:25	79:21
1g$^+BF_4^-$	4-$C_6H_4OCH_3$	*c*	74:26

[a] 0.00071 M (293 K) in CH_2Cl_2. [b] Values are from $^{31}P\{^1H\}$ NMR spectra and are the averages of at least four runs, with S/N ranges of (π:π', 183 K/173 K) **a**, 70−238:3−8/69−300:3−8; **b**, 100−217:15−27/33−190:5−24; **c**, 39−114:7−22/43−249:8−47; **d**, 124−210:34−49/25−209:5−48; **e**, 43−84:14−28/29−98:9−30; **f**, 14−109:5−32/29−167:8−46; **g**, −/6−33:2−10, as summarized in the supporting information. Standard deviations on each integer of the normalized ratios are (183 K/173 K) **a**, 0.3/0.4; **b**, 0.5/0.6; **c**, 0.5/0.5; **d**, 0.3/0.6; **e**, 0.6/0.5; **f**, 0.6/1.0; **g**, −/1.7. [c] The temperature is close to T_c.

Table 3. Effect of Concentration upon Aldehyde Binding Selectivities[a]

1e$^+BF_4^-$, M	π/π'	
(CH_2Cl_2, 293 K)	183 K	173 K
0.000709	73:27	76:24
0.00743	77:23	79:21
0.0179	79:21	81:19
0.0558	81:19	83:17
0.156	83:17	85:15

[a] Values are from $^{31}P\{^1H\}$ NMR spectra, one run.

Table 4. Effect of Counteranion and Configuration upon Aldehyde Binding Selectivities under "Standard Conditions" [a]

	π/π'	
compd	183 K	173 K
1c$^+BF_4^-$	83:17	84:16
1c$^+PF_6^-$	80:20	81:19
(+)-(*R*)-**1d**$^+BF_4^-$	78:22[b]	80:20
1d$^+BF_4^-$	78:22	80:20
1d$^+PF_6^-$	74:26	76:24
1d$^+SbF_6^-$	73:27	76:24
1e$^+BF_4^-$	73:27	76:24
1e$^+PF_6^-$	70:30	74:26

[a] 0.00071 M (293 K) in CH_2Cl_2 and from two−four independently prepared samples as described in Table 2. [b] This ratio increased to 85:15 in a sample that was 0.076 M in CD_2Cl_2.

standard concentration) of *p*-methylbenzaldehyde complex **1e**$^+BF_4^-$ were recorded at 203, 193, 183, and 173 K. As summarized in Table 5, binding selectivities were slightly higher at lower temperatures.[20] Similar results were obtained with benzaldehyde complex **1d**$^+BF_4^-$ in the lower freezing solvent $CHCl_2F$ (Table 5).[22] The *p*-methoxybenzaldehyde complex **1g**$^+BF_4^-$ gave parallel trends. However, the π/π' ratios of

Table 5. Effect of Temperature upon Aldehyde Binding Selectivities

temp (K)	**1e**$^+BF_4^-$ π/π' (CH_2Cl_2)[a,b]	**1d**$^+BF_4^-$ π/π' ($CHCl_2F$)[b,c]
203	72:28	
193	74:26	
183	74:26	76:24
173	76:24	78:22
163		82:18
153		83:17

[a] 0.0074 M (293 K). [b] Values are from $^{31}P\{^1H\}$ NMR spectra, one run. [c] 0.00071 M (293 K).

fluorinated aldehyde complexes **1a**,**b**$^+BF_4^-$ did not vary outside of experimental error between 273 and 173 K.[23] These compounds give higher π/π' ratios, and thus slight changes are more difficult to quantify.

4. Crystal Structures of Aromatic Aldehyde Complexes. The preceding compounds, and other aromatic aldehyde complexes of **I**, were subjected to an extensive series of crystallizations.[24] X-ray data were collected at room temperature (**1a**−**c**,**f**$^+PF_6^-$, **1d**$^+SbF_6^-$) and low temperature (**1a**,**c**,**f**$^+PF_6^-$, **1d**$^+SbF_6^-$) as outlined in Table 6. Refinements are detailed in the Experimental Section. Each complex crystallized as the more stable π (*RS*,*SR*) diastereomer. The O=CH hydrogen atoms of (*RS*,*SR*)-**1a**−**c**,**f**$^+PF_6^-$ were located, and the methyl group of (*RS*,*SR*)-**f**$^+PF_6^-$ was disordered (Experimental Section). The *p*-methoxybenzaldehyde complex **1g**$^+PF_6^-$ crystallized as a σ isomer, the structure of which is reported elsewhere.[7d]

Figure 2 shows two views of a representative cation and an overlay of all cations. Additional structures are given in the supporting information, together with atomic coordinates, selected bond lengths and angles, torsion angles, and anisotropic thermal parameters. Key features of the cations are illustrated in Chart 2.

Consider first the five structures determined at room temperature (16 °C). Importantly, the rhenium−carbon bond lengths increase monotonically from 2.161(9) Å ((*RS*,*SR*)-**1a**$^+PF_6^-$) to 2.199(6) Å ((*RS*,*SR*)-**1f**$^+PF_6^-$) as the π/π' ratios in Table 2 decrease. This correlation is plotted and carefully

(22) Siegel, J. S.; Anet, F. A. L. *J. Org. Chem.* **1988**, *53*, 2629.

(23) Area ratios of cyclopentadienyl $^1H/PPh_3$ ^{31}P resonances (π:π'): **1a**$^+BF_4^-$ (0.062 M) 96:4/96:4 (273 K), 97:3/96:4 (253 K), 98:2/97:3 (233 K), 97:3 (203 K)/98:2 (213 K), 98:2 (173 K)/97:3 (183 K); **1b**$^+BF_4^-$ (0.13 M) −/90:10 (263 K), 90:10/89:11 (243 K), 90:10/89:11 (223 K), 91:9/91:9 (203 K), 92:8/90:10 (183 K).

(24) Optimally, correlations between solution and solid state phenomena should use as many data points as possible. Over a four year period, we prepared complexes of **I** and a variety of substituted benzaldehydes (e.g., *p*-azido, *p*-phenyl, *p*-fluoro, *p*-chloromethyl, *p*-iodomethyl, *p*-methoxymethyl, *p*-phenoxy, *p*-trimethylsilyl, *p*-dimethylphenylsilyl, *p*-trimethylstannyl, *p*-triphenylstannyl), and attempted numerous crystallizations. However, only the five compounds in Chart 2 gave material suitable for X-ray analysis. Crystals of (−)-(*SR*)-**1d**$^+BF_4^-$ and (−)-(*SR*)-**1d**$^+PF_6^-$ yielded data of extremely poor quality due either to severe disorder or the presence of more than one independent molecule in the unit cell.

Table 6. Summary of Crystallographic Data for π Aromatic Aldehyde Complexes (*RS*,*SR*)-[(η^5-C_5H_5)Re(NO)(PPh_3)(η^2-O═CHAr)]$^+X^-$; ((*RS*,*SR*)-**1**$^+X^-$; Ar = **a**, C_6F_5; **b**, 4-$C_6H_4CF_3$; **c**, 4-C_6H_4Cl; **d**, C_6H_5; **f**, 4-$C_6H_4CH_2CH_3$)

compound	(*RS*,*SR*)-**1a**$^+PF_6^-$		(*RS*,*SR*)-**1b**$^+PF_6^-$	(*RS*,*SR*)-**1c**$^+PF_6^-$		(*RS*,*SR*)-**1d**$^+SbF_6^-$		(*RS*,*SR*)-**1f**$^+PF_6-$	
molecular formula	$C_{30}H_{21}F_{11}NO_2P_2Re$		$C_{31}H_{25}F_9NO_2P_2Re$	$C_{30}H_{25}ClF_6NO_2P_2Re$		$C_{30}H_{26}F_6NO_2PSbRe$		$C_{32}H_{30}F_6NO_2P_2Re$	
molecular weight	884.638		862.684	829.131		885.462		822.740	
crystal system	monoclinic		triclinic	triclinic		monoclinic		monoclinic	
space group	$P2_{1/n}$ (no. 14)		$P\bar{1}$ (no. 2)	$P\bar{1}$ (no. 2)		$P2_1/c$ (no. 14)		$P2_1/n$ (no. 14)	
temp of collection (°C)	−80	16	16	−125	16	−80	16	−80	16
cell dimensions									
a, Å	13.743(5)	13.775(1)	14.908(2)	10.588(1)	10.584(2)	11.728(5)	11.790(2)	13.600(2)	13.690(1)
b, Å	16.024(2)	16.247(1)	10.656(1)	14.789(2)	14.987(1)	17.997(4)	18.160(2)	21.709(3)	21.844(2)
c, Å	15.188(5)	15.196(1)	10.220(1)	9.810(1)	9.958(1)	14.225(2)	14.357(2)	10.701(1)	10.781(1)
α, deg			95.38(2)	107.08(1)	106.89(1)				
β, deg	116.54(2)	116.360(3)	74.74(2)	94.99(1)	93.55(1)	100.95(2)	100.72(1)	105.77(1)	106.00(1)
γ, deg			93.64(2)	84.46(1)	85.67(1)				
V, Å^3	2992.18	3047.31	1558.29	1459.63	1505.81	2947.83	3020.18	3040.27	3099.00
Z	4	4	2	2	2	4	4	4	4
d_{calc}, g/cm^3	1.96	1.93	1.84	1.89	1.83	2.00	1.95	1.80	1.76
d_{obs}, g/cm^3 (CCl_4/CH_2I_2)	densities were determined at −16°	1.92	1.83	densities were determined at −16°	1.82	densities were determined at −16°	1.92	densities were determined at −16°	1.74
crystal dimensions, mm	0.36 × 0.36 × 0.09	0.38 × 0.23 × 0.17	0.23 × 0.22 × 0.08	0.25 × 0.19 × 0.09	0.22 × 0.16 × 0.13	0.27 × 0.25 × 0.17	0.28 × 0.28 × 0.05	0.32 × 0.29 × 0.07	0.31 × 0.22 × 0.09
diffractometer	Enraf-Nonius CAD-4	Syntex P$\bar{1}$	Syntex P$\bar{1}$	Syntex P$\bar{1}$	Enraf-Nonius CAD-4	Enraf-Nonius CAD-4	Syntex P$\bar{1}$	Enraf-Nonius CAD-4	Enraf-Nonius CAD-4
radiation (*λ*, Å)	Mo Kα (0.71073)	Mo Kα (0.71073)	Mo Kα (0.71073)	Cu Kα (1.54056)	Cu Kα (1.54056)	Mo Kα (0.71073)	Mo Kα (0.71073)	Mo Kα (0.71073)	Cu Kα (1.54056)
data collection method	$\theta-2\theta$	$\theta-2\theta$	$\theta-2\theta$	$\theta-2\theta$	$\theta-2\theta$	$\theta-2\theta$	$\theta-2\theta$	$\theta-2\theta$	$\theta-2\theta$
scan speed, deg/min	variable, 1−8	variable, 3−8	3.0	variable, 1−8	variable, 1−8	variable, 1−8	3.0	variable, 1−8	variable, 1−8
reflections measured	5687	5318	5658	5193	5317	5609	4684	5749	5207
range/indices (*hkl*)	0,16 0,18 −17,16	0,15 0,18 −16,16	0,12 −12,12 −12,12	0,12 −17,17 −11,11	0,12 −17,17 −11,11	0,13 0,21 −16,16	0,12 0,19 −15,15	0,16 0,25 −12,12	0,16 0,21 −10,10
scan range	0,80 + 0.35(tanθ)	$k_{\alpha1}$ −1.3 to $k_{\alpha2}$ +1.6	$k_{\alpha1}$ −1.0 to $k_{\alpha2}$ +1.0	0.80 + 0.14(tan θ)	0.80 + 1.40(tan θ)	0.80 + 0.34(tan θ)	$k_{\alpha1}$ −1.0 to $k_{\alpha2}$ + 1.0	0.80 + 0.34(tan θ)	0.80 + 1.40 (tan θ)
2θ limit, deg	4.0−50.0	3.0−48.0	3.0−48.0	4.0−130.0	4.0−130.0	4.0−50.0	3.0−46.0	4.0−50.0	4.0−130.0
time between std	1 X-ray hour	98 reflections	98 reflections	1 X-ray hour	1 X-ray hour	1 X-ray hour	98 reflections	1 X-ray hour	1 X-ray hour
total no. of unique data	5232	4998	5458	4980	5023	5148	4366	5341	4447
no. of observed data, $I > 3\sigma(I)$	3881	2994	4508	4713	4729	4220	2677	4168	4202
abs coefficient, cm^{-1}	43.18	42.40	41.35	103.89	100.69	52.01	50.76	42.206	89.78
min transmission, %	47.01	67.21	92.63	45.14	75.77	55.93	79.67	57.62	29.55
max transmission, %	99.96	99.43	108.17[a]	99.68	99.80	99.92	130.91[a]	99.87	99.92
no. of variables	507	428	415	388	389	379	379	410	398
goodness of fit	1.18	1.15	1.60	0.91	1.59	1.39	2.55	1.13	1.11
R (averaging) (I_{obs}, F_{obs})	0.015, 0.012	0.026, 0.017		0.023, 0.014	0.024, 0.017	0.027, 0.028	0.042, 0.023	0.020, 0.014	0.029, 0.018
$R = \sum\|\|F_o\| - \|F_c\|\|/\sum\|F_o\|$	0.026	0.034	0.029	0.028	0.031	0.032	0.036	0.026	0.031
$R_w = \sum\|\|F_o\| - \|F_c\|\|w^{1/2}/\sum\|F_o\|w^{1/2}$	0.037	0.044	0.032	0.032	0.034	0.040	0.042	0.032	0.034
Δ/σ (max)	0.004	0.006	0.011	0.001	0.001	0.002	0.006	0.004	0.011
$\Delta\rho$ (max), e/Å^3	1.02 (0.9 Å from Re)	1.55 (1.22 Å from Re)	0.74 (3.4 Å from Re)	1.30 (1.01 Å from C6)	0.87 (0.74 Å from Re)	1.03 (1.313 Å from Re)	0.67	0.83	0.69

[a] The program DIFABS was utilized for the absorption corrections.

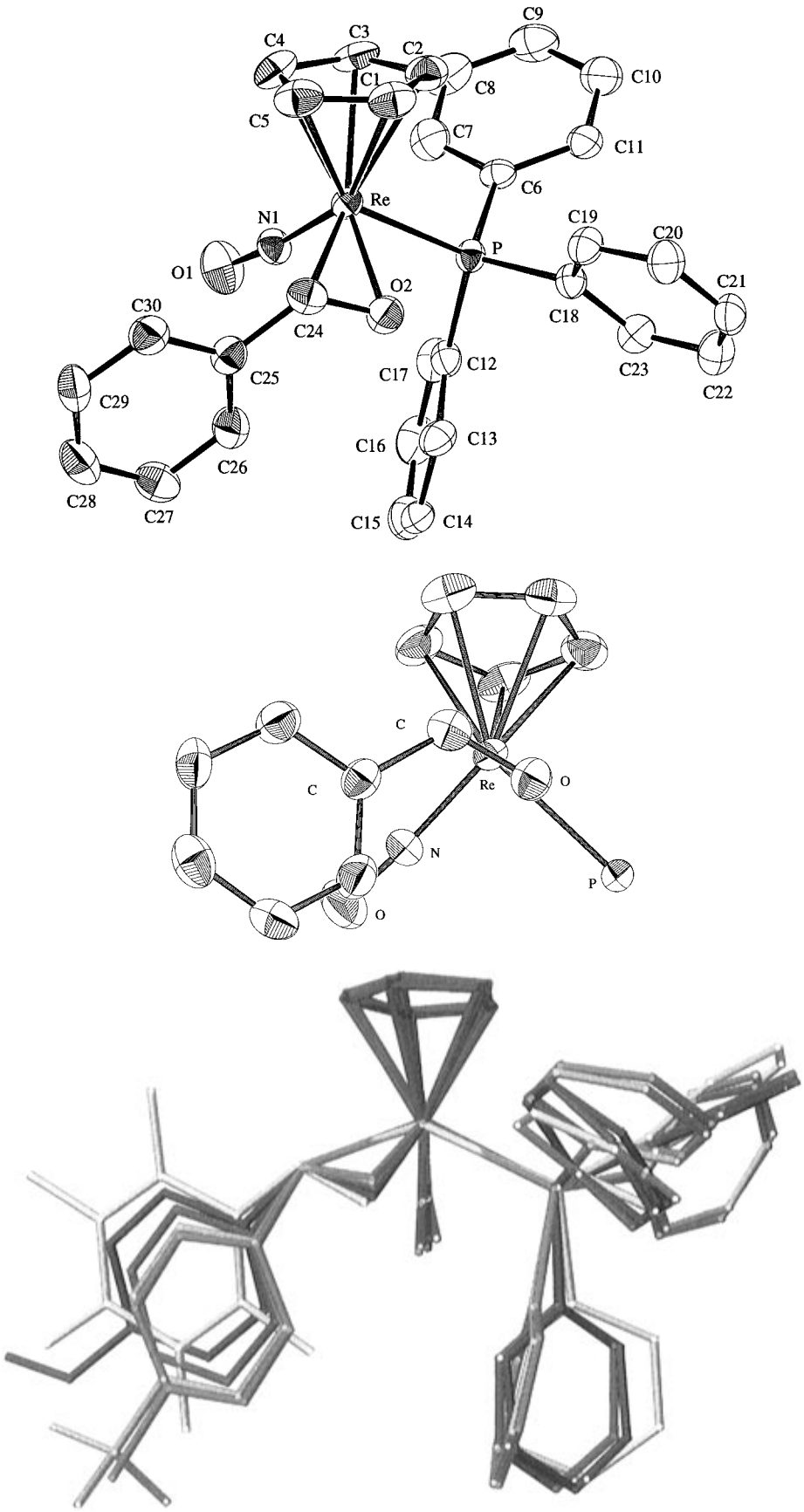

Figure 2. Representative structures: top, cation of benzaldehyde complex (*RS*,*SR*)-**1d**$^+SbF_6^-$ (−80 °C); middle, Newman-type projection with PPh_3 phenyl rings omitted; bottom, overlay of cations of (*RS*,*SR*)-**1a**−**d**,**f**$^+X^-$ (16 °C). This figure, presented here in black and white, is available in color on the World Wide Web. See Supporting Information paragraph on any current masthead page for instructions on accessing the images.

examined from a statistical viewpoint below. The four structures determined at low temperature show a similar trend. In three cases, the rhenium−carbon bonds *appear* to very slightly or moderately contract at low temperature ((*RS*,*SR*)-**1a**$^+PF_6^-$, (*RS*,*SR*)-**1d**$^+SbF_6^-$, (*RS*,*SR*)-**1f**$^+PF_6^-$). As is often observed, the unit cell volumes decrease by 2−3% at low temperature.

In all cases, the rhenium−oxygen bonds (2.046(3)−2.083(5) Å) are shorter than the rhenium−carbon bonds. Since

Chart 2. Views of the Re-O=C Planes of π Aromatic Aldehyde Complexes (*RS,SR*)-**1a**−**d**,**f**$^+$X$^-$ and Key Structural Parameters

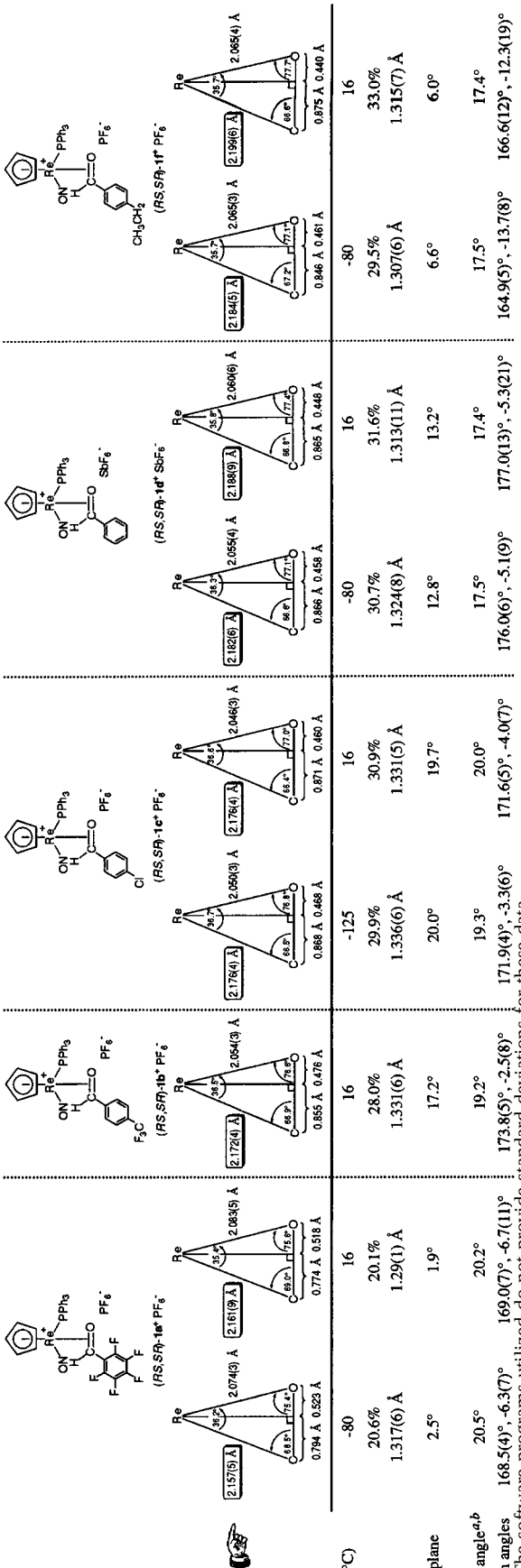

collection temp (°C)	-80	16	16	-125	16	-80	16	-80	16
slippage[a]	20.6%	20.1%	28.0%	29.9%	30.9%	30.7%	31.6%	29.5%	33.0%
O=C bond angle, Re-O=C plane with Re-P bond[b]	1.317(6) Å 2.5°	1.29(1) Å 1.9°	1.331(6) Å 17.2°	1.336(6) Å 20.0°	1.331(5) Å 19.7°	1.324(8) Å 12.8°	1.313(11) Å 13.2°	1.307(6) Å 6.6°	1.315(7) Å 6.0°
OC-C bend-back angle[a,b]	20.5°	20.2°	19.2°	19.3°	20.0°	17.5°	17.4°	17.5°	17.4°
O=C-C=C torsion angles	168.5(4)°, -6.3(7)°	169.0(7)°, -6.7(11)°	173.8(5)°, -2.5(8)°	171.9(4)°, -3.3(6)°	171.6(5)°, -4.0(7)°	176.0(6)°, -5.1(9)°	177.0(13)°, -5.3(21)°	164.9(5)°, -13.7(8)°	166.6(12)°, -12.3(19)°

[a] See text.[26] [b] The software programs utilized do not provide standard deviations for these data.

carbon is less electronegative and can better support a partial positive charge, the rhenium "slips" toward oxygen. Analogous phenomena have previously been observed and analyzed in alkene complexes.[25] A slippage parameter can be defined,[26] which exhibits a general upward trend as the π/π' ratios increase (Chart 2). However, except for the rhenium−carbon bond lengths, no other geometric features of the Re-O=C units exhibit monotonic trends. For example, the oxygen−carbon bond lengths (1.29(1)−1.336(6) Å)[27] do not vary in a regular fashion. Possible rationales are discussed below.

In the idealized π isomers **II** and **IV** (Chart 1/Scheme 1), the Re-O=C planes and Re−P bonds make 0° angles. As analyzed above, this maximizes overlap of the d orbital HOMO of **I** and the ligand O=C π* acceptor orbital. Significantly, the angle in pentafluorobenzaldehyde complex (*RS,SR*)-**1a**$^+$PF$_6^-$, which has the strongest π accepting ligand, is closest to ideality (2.5−1.9°). The angles in the remaining complexes show larger, counterclockwise deviations (6.0−20.0°), but not in any regular trend. As is also expected from d/π* orbital interactions, the OC−C bonds bend out of the π nodal planes of the free aldehydes. "Bend back angles" can be calculated[6c] and are similar in all complexes (20.5−17.4°). The O=C−C··C torsion angles are also similar (165° to 177° and −14° to −3°), indicating comparable conformations about the OC−C bonds. This is nicely illustrated in the overlaid structures in Figure 2.

The overlaid structures also suggest a factor that may contribute to the lack of monotonic trends in some of the above geometric parameters. Specifically, *p*-trifluoromethylbenzaldehyde and *p*-chlorobenzaldehyde complexes (*RS,SR*)-**1b**,**c**$^+$-PF$_6^-$ crystallize with PPh$_3$ conformations that differ from the others. Further, the propeller chirality[28] is opposite to those of all π aldehyde complexes of **I** that have been structurally characterized to date.[6a,c,9c,29] This variable does not disrupt the

(25) (a) Eisenstein, O.; Hoffmann, R. *J. Am. Chem. Soc.* **1981**, *103*, 4308. (b) Cameron, A. D.; Smith, V. H. Jr.; Baird, M. C. *J. Chem. Soc., Dalton Trans.* **1988**, 1037. (c) The crystal structures of three closely related platinum(II) *p*-nitrostyrene, styrene, and *p*-dimethylaminostyrene complexes have been determined. Although the standard deviations are somewhat high, the Pt−CHAr bond lengths appear to increase monotonically from 2.216(11) to 2.236(10) to 2.262(16) Å. The Pt−CH$_2$ and H$_2$C=CHAr bond lengths vary irregularly (2.174(13)/1.374(18), 2.180(12)/1.454(17), 2.137(17)/1.419(25) Å). Nyburg, S. C.; Simpson, K.; Wong-Ng, W. *J. Chem. Soc., Dalton Trans.* **1976**, 1865.

(26) The slippage value is 0% when the perpendicular from rhenium to the O=C bond intercepts the midpoint, as in an equilateral triangle. At the other limit, the slippage value is 100% when the perpendicular intersects the oxygen or carbon atom.

(27) As expected from backbonding, the oxygen−carbon bond lengths are between those of single and double bonds. Crystal structures of only two other π aromatic aldehyde complexes have been reported, (η^5-C$_5$H$_5$)W(CO)(η^2-NH(CH$_3$)=C(Ar)Ar′)(η^2-O=CHC$_6$H$_5$) and (Me$_3$P)$_2$W(=S)$_2$(η^2-O=CHC$_6$H$_5$) (O=C 1.333(12) and 1.376 (9) Å): (a) Brunner, H.; Wachter, J.; Bernal, I.; Creswick, M. *Angew. Chem., Int. Ed. Engl.* **1979**, *18*, 861. (b) Creswick, M. W.; Bernal, I. *Inorg. Chim. Acta* **1983**, *71*, 41. (c) Rabinovich, D.; Parkin, G. *J. Am. Chem. Soc.* **1991**, *113*, 5904.

(28) (a) Brown, J. M.; Mertis, K. *J. Organomet. Chem.* **1973**, *47*, C5. (b) Gust, D.; Mislow, K. *J. Am. Chem. Soc.* **1973**, *95*, 2854. (c) Faller, J. W.; Johnson, B. V. *J. Organomet. Chem.* **1975**, *96*, 99. (d) Bye, E.; Schweizer, B.; Dunitz, J. D. *J. Am. Chem. Soc.* **1982**, *104*, 5893. (e) Brunner, H.; Hammer, B.; Krüger, C.; Angermund, K.; Bernal, I. *Organometallics* **1985**, *4*, 1063. (f) Davies, S. G.; Derome, A. E.; McNally, J. P. *J. Am. Chem. Soc.* **1991**, *113*, 2854. (g) Polowin, J.; Mackie, S. C.; Baird, M. C. *Organometallics* **1992**, *11*, 3724. (h) Garner, S. E.; Orpen, A. G. *J. Chem. Soc., Dalton Trans.* **1993**, 533. (i) Brunner, H.; Oeschey, R.; Nuber, B. *Angew. Chem., Int. Ed. Engl.* **1994**, *33*, 866.

(29) This generalization also includes π formaldehyde, thioformaldehyde, selenoformaldehyde, and 1,3-difluoroacetone adducts of **I**: (a) Buhro, W. E.; Georgiou, S.; Fernández, J. M.; Patton, A. T.; Strouse, C. E.; Gladysz, J. A. *Organometallics* **1986**, *5*, 956. (b) Buhro, W. E.; Etter, M. C.; Georgiou, S.; Gladysz, J. A.; McCormick, F. B. *Organometallics* **1987**, *6*, 1150. (c) McCormick, F. B. *Organometallics* **1984**, *3*, 1924. (d) Klein, D. P.; Dalton, D. M.; Quirós Méndez, N.; Arif, A. M.; Gladysz, J. A. *J. Organomet. Chem.* **1991**, *412*, C7.

Chart 3. Views of the Re-O=C Planes of π Aliphatic Aldehyde Complexes (*RS*,*SR*)-[(η^5-C_5H_5)Re(NO)(PPh$_3$)(η^2-O=CHR)]$^+PF_6^-$ ((*RS*,*SR*)-**2**$^+PF_6^-$) and Key Structural Parameters

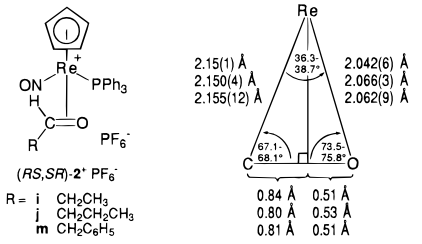

slippage[a]	24% / 20% / 23%
O=C bond	1.35(1) Å / 1.338(5) Å / 1.318(11) Å
angle, Re-O=C plane with Re-P bond[b]	17.0° / 20.5° / 22.8°
OC-R bend-back angle[a,b]	19.2° / 19.3° / 19.0°
O=C-C-R torsion angle	76.8(16)° / 77.2(6)° / 94.5°[b]

[a] See text. [b] The software programs utilized do not provide standard deviations for these data.

electronic effect upon the lengths of the remote rhenium−carbon bonds. However, trends involving the closer oxygen may be affected.[30] Such conformational isomers rapidly interconvert in solution,[28f,i] and equilibrium ratios should be similar for all complexes. Regardless, **I** should not be viewed as a rigid chiral receptor, and the π/π' ratios (Tables 2−4) reflect an ensemble of equilibrium constants involving all significantly populated conformations.

5. Aliphatic Aldehyde Complexes. Similar binding selectivity data were sought for the π aliphatic aldehyde complexes [(η^5-C_5H_5)Re(NO)(PPh$_3$)(η^2-O=CHR)]$^+BF_4^-$ (**2**$^+BF_4^-$; R = **h**, CH_3; **i**, CH_2CH_3; **j**, $CH_2CH_2CH_3$; **k**, $CH(CH_3)_2$; **l**, $C(CH_3)_3$).[6a,c] The crystal structures of propionaldehyde and butyraldehyde complexes (*RS*,*SR*)-**2i**,**j**$^+PF_6^-$, and the corresponding phenylacetaldehyde complex (*RS*,*SR*)-**2m**$^+PF_6^-$, have been reported earlier.[6a,c] All exhibit comparable metrical parameters, as summarized in Chart 3.

When ^{31}P and ^{1}H NMR spectra of acetaldehyde, propionaldehyde, and butyraldehyde complexes **2h**−**j**$^+BF_4^-$ were recorded at low temperature in CD_2Cl_2 (0.011−0.015 M), the PPh$_3$ and cyclopentadienyl resonances of the π/π' isomers decoalesced. Typical spectra are given in Figure 1 (bottom). As compiled in Table 7, π/π' ratios (173 K) increased from 99.0:1.0 for **2h**$^+BF_4^-$ to 99.8−99.5:0.2−0.5 for **2i**,**j**$^+BF_4^-$. Isobutyraldehyde and pivalaldehyde complexes **2k**,**l**$^+BF_4^-$, which bear branched O=C substituents, did not show any evidence for π' isomers. As little as 0.1% would have been detected.

All π/π' ratios were assayed from 500 MHz ^{1}H NMR spectra of three to four independently prepared samples. Since it is easier to determine the relative areas of comparably-sized peaks, the *down*field ^{13}C satellites of the cyclopentadienyl resonances of the π isomers were integrated versus the cyclopentadienyl resonances of the π' isomers. The π/π' ratios were then calculated assuming a 100:0.55 resonance/satellite area ratio. Spinning side bands often interfered (Figure 1, bottom right). Thus, spin rates were varied to confirm peak assignments, and spectra were recorded without spinning. The latter gave identical π/π' ratios. As a further check, the ^{31}P resonances were also integrated. Each component of each π/π' ratio was within ±0.1 of those in Table 7.

Table 7. Summary of NMR Data and Binding Selectivities for Diastereomeric π Aliphatic Aldehyde Complexes [(η^5-C_5H_5)Re(NO)(PPh$_3$)(η^2-O=CHR)]$^+BF_4^-$ (**2**$^+BF_4^-$)[a]

		NMR (π/π'; 173 K)		
compd	R	^{31}P{^{1}H} (ppm)	^{1}H (δ, C_5H_5)	ratio[b]
2h$^+BF_4^-$	CH_3	11.2/10.5	5.86/5.77	99.0/1.0
2i$^+BF_4^-$	CH_2CH_3	11.2/10.3	6.01/5.90	99.8/0.2
2j$^+BF_4^-$	$CH_2CH_2CH_3$	11.3/10.3	6.01/5.90	99.5/0.5
2k$^+BF_4^-$	$CH(CH_3)_2$	11.1/[c]	5.92/[c]	>99.9/<0.1
2l$^+BF_4^-$	$C(CH_3)_3$	11.0/[c]	5.92/[c]	>99.9/<0.1

[a] 0.011−0.015 M (293 K) in CD_2Cl_2. [b] Values are from 500 MHz ^{1}H NMR spectra and are the averages of three-four runs. Standard deviations on each component of the normalized ratios are **h**, 0.08; **i**, 0.01; **j**, 0.08. [c] Not observed.

As with **1a**−**g**$^+BF_4^-$, the cyclopentadienyl ^{1}H resonances of the π' isomers of **2h**−**j**$^+BF_4^-$ were upfield of those of the π isomers. However, as illustrated in Figure 1, the chemical shift differences were less. This follows plausibly from aryl group shielding effects noted above. Interestingly, the ^{31}P chemical shift trends were reversed. Although additional supporting data for the structural assignments would be desirable, the propene complex of **I** similarly gives a higher π/π' equilibrium ratio than the styrene complex (see below).[8b] In view of the difficulties in quantifying small differences in high π/π' ratios, concentration, counteranion, and temperature effects were not examined.

Discussion

1. Effect of Ligand upon Binding Selectivities. The data in Table 2 establish a marked electronic effect upon thermodynamic enantioface binding selectivities in adducts of aromatic aldehydes and the chiral rhenium Lewis acid **I**. The more π acidic aldehydes show distinctly higher chiral recognition, with $\Delta G_{173\ K}$ values for π/π' isomers decreasing from 1.20 kcal/mol for pentafluorobenzaldehyde complex **1a**$^+BF_4^-$ to 0.36 kcal/mol for *p*-methoxybenzaldehyde complex **1g**$^+BF_4^-$. The Hammett plots of log (K/K_o) vs σ in Figure 3 further support the electronic origin of this trend. Although a σ value is not available for the pentafluorophenyl group, the other six complexes give quite good linear correlations, with slopes (ρ) of 0.60 (183 K, R = 0.997) and 0.46 (173 K, R = 0.984). As gauged by either σ or σ^+ values, a *p*-ethyl group is slightly *less* electron-releasing than a *p*-methyl group. Accordingly, the π/π' ratio for **1f**$^+BF_4^-$ is greater than that of **1e**$^+BF_4^-$.[32]

The data in Chart 2 establish the underlying structural basis for this phenomenon. As the rhenium−carbon bonds extend from 2.157(5)−2.161(9) Å in pentafluorobenzaldehyde complex (*RS*,*SR*)-**1a**$^+PF_6^-$ to 2.184(5)−2.199(6) Å in *p*-ethylbenzalde-

(30) A reviewer has made several additional perceptive points. First, for free aromatic aldehydes, electron withdrawing aryl substituents should give *shorter* oxygen−carbon bonds.[31a] Since backbonding is in turn stronger for aldehyde ligands with electron withdrawing substituents, the oxygen−carbon bond lengths in (*RS*,*SR*)-**1a-d**,**f**$^+X^-$ may be less sensitive to substituents. Thus, the *differences* between the oxygen−carbon bond lengths of the free and coordinated aldehydes would be more likely to exhibit a monotonic trend. Also, electron donating substituents make the aldehyde oxygen a stronger donor, while electron withdrawing substituents make the oxygen a stronger acceptor. This may dampen variations in rhenium−oxygen bond lengths. Further, computational studies of carbonyl compounds X(H)C=O show that carbon atom charges vary greatly with X, whereas oxygen atom charges vary only slightly.[31a,b] Finally, relationships between metal−carbon, metal−oxygen, and oxygen−carbon bond lengths have also been experimentally and theoretically investigated in η^2-acyl complexes.[31c,d]

(31) (a) Structural data do not appear to be available for the free aldehyde ligands of **1a**−**d**,**f**$^+X^-$. However, analogous trends are well established for other types of carbonyl compounds: Wiberg, K. B.; Hadad, C. M.; Rablen, P. R.; Cioslowski, J. *J. Am. Chem. Soc.* **1992**, *114*, 8644. (b) Rosenberg, R. E. Jr. *J. Am. Chem. Soc.* **1995**, *117*, 10358. (c) Curtis, M. D.; Shiu, K.-B.; Butler, W. M. *J. Am. Chem. Soc.* **1986**, *108*, 1550. (d) Durfee, L. D.; Rothwell, I. P. *Chem. Rev.* **1988**, *88*, 1059.

(32) (a) In contrast, the ($\pi+\pi'$)/σ ratios (which usually parallel π/π' ratios) show an opposite trend (**1e**$^+BF_4^-$ > **1f**$^+BF_4^-$; Scheme 1). (b) As would also be expected for an electronic effect, the π/π' ratios of **1a**−**e**,**g**$^+BF_4^-$ decrease as the IR ν_{NO} values[7d] decrease over the narrow range 1745−1735 cm^{-1}.

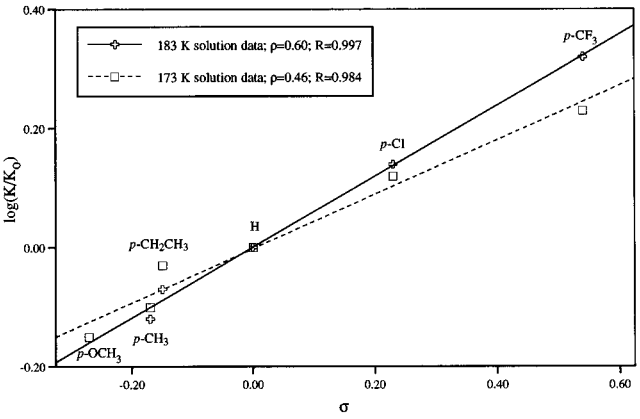

Figure 3. Hammett plot of equilibrium constants for π/π' isomers of aromatic aldehyde complexes **1b**−**g**$^+BF_4^-$ under "standard conditions".

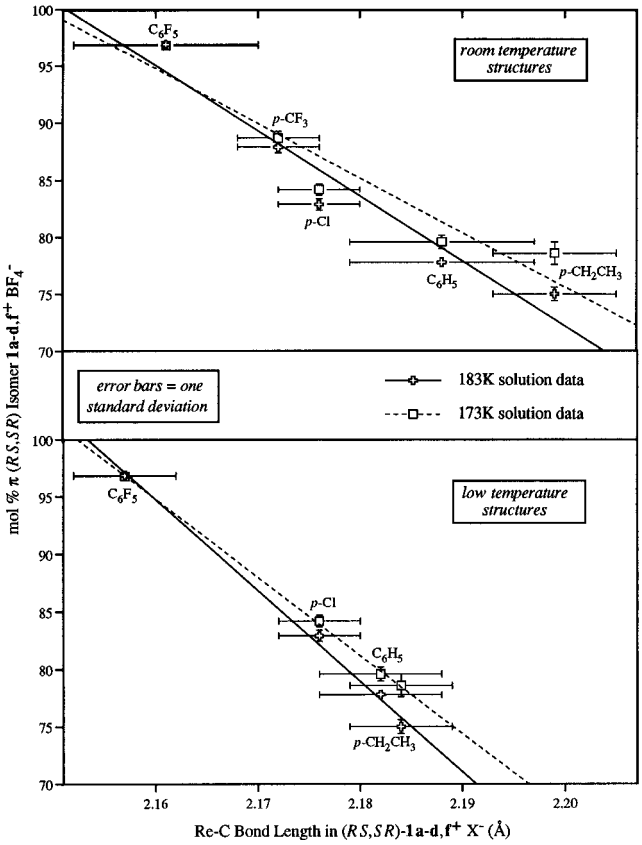

Figure 4. A crystallographic "map" of chiral recognition in aromatic aldehyde complexes **1a**−**d**,**f**$^+X^-$.

hyde complex (*RS*,*SR*)-**1f**$^+PF_6^-$, the enantioface binding selectivities (Table 2) drop from 97:3 to 79−76:21−24.[15] This trend reflects diminished steric interactions between the O═CH***Ar*** moieties and cyclopentadienyl ligands in the less stable π' isomers. These data are plotted in Figure 4, which can be regarded as a crystallographic "map" of chiral recognition. For clarity, the room temperature and low temperature rhenium−carbon bond lengths are graphed separately.

The data in Figure 4 are shown with error bars corresponding to one standard deviation. These range from ±0.3 to ±1.7 for the mol% of the π isomer and from ±0.004 to ±0.009 Å for the rhenium−carbon bond lengths. By the commonly employed "three standard deviation" criterion, the bond lengths in adjacent pairs of compounds are not significantly different. Nonetheless, there is a statistically rigorous correlation with the π/π' ratios in solution. For example, the commonly utilized χ^2 test can be applied. If, as a simplification, a linear relationship is assumed, the probability that the data are random as opposed to correlated is less than 5%.[33]

The data in Table 7 establish a complementary steric effect upon enantioface binding selectivities of aliphatic aldehydes. The π/π' ratios increase as the sizes of the O═CH***R*** substituents increase from methyl (99.0:1.0) to *n*-alkyl (99.5−99.8:0.5−0.2) to *sec*- or *tert*-alkyl (>99.9:<0.1). Surprisingly, propionaldehyde reproducibly gives a higher π/π' ratio than butyraldehyde. Although we presently lack a rationale for this trend, the difference is slight.

Aliphatic aldehydes also bind much more selectively to **I** than aromatic aldehydes. From the three crystal structures of aliphatic aldehyde complexes in Chart 3, an "average" rhenium−carbon bond length of 2.15 Å can be confidently assigned. When this value is extrapolated on the plots in Figure 4, >99:<1 equilibrium mixtures of π/π' isomers are predicted. Although this is in good agreement with experiment, there are several hints that the correlation may be fortuitous.

For example, similar trends occur with monosubstituted alkene complexes of **I**. Representative enantioface binding selectivities are summarized in Scheme 2.[8b,9a,b,10c,34] The π/π' ratios for alkenes with sp^3-hybridized substituents (**VI**/**VII**) are *higher* than those with sp^2-hybridized phenyl, vinyl, or carbonyl substituents (**VIII**/**IX**). However, crystal structures do not show any obvious bond length trends.[8a,b,g,9a,b,10a,b]

Thus, other factors may contribute to the lower binding selectivities of aromatic vs aliphatic aldehydes. For example, "flatter" sp^2-hybridized O═C substituents might experience less steric interactions with the cyclopentadienyl ligands in the π' isomers. Alternatively, there is an increasing body of data suggesting *attractive* interactions between the "edges" or carbon−hydrogen bonds of cyclopentadienyl ligands and π clouds of unsaturated moities.[35] This could slightly stabilize the π' isomers. Regardless, geminally disubstituted alkenes such as α-methyl styrene provide useful probes.[10c] This ligand must direct either a methyl *or* phenyl substituent toward the cyclopentadienyl ligand. The isomer with the phenyl group *syn* is favored (**X**, Scheme 2).[10c,36]

A glyoxal complex of **I** has been prepared[9c] and exists as a 95:5 mixture of π/π' isomers over a wide range of temperatures and concentrations in CH_2Cl_2 (Scheme 3).[34] However, the crystal structure of the π isomer shows a rhenium−carbon bond (2.129(5) Å) even shorter than those in (*RS*,*SR*)-**2i**,**j**,**m**$^+PF_6^-$ (Chart 3). Thus, an sp^2-hybridized substituent again results in an abnormally low binding selectivity. A O═C-ligated acrolein complex of **I** has also been prepared.[9a] Curiously, this approximately isosteric compound exists as a >99:<1 mixture of π/π' isomers (Scheme 3). Hence, additional factors (presumably electronic) must affect this equilibrium.

2. Other Binding Selectivity Issues. Binding selectivities usually increase at lower temperatures. Thus, the modest rise in π/π' ratios as temperatures decrease, as documented in Table 5 and elsewhere, is not surprising.[20b] However, we do not presently have a rationale for the counteranion effects in Table

(33) Barlow, R. *Statistics*; Wiley: New York, 1989; Chapter 8.3.1.

(34) All data in Schemes 2 and 3 are for BF_4^- salts.

(35) (a) Brunner, H. *Angew. Chem., Int. Ed. Engl.* **1983**, *22*, 897; see sections 6−8. (b) Nishio, M.; Umezawa, Y.; Hirota, M.; Takeuchi, Y. *Tetrahedron* **1995**, *51*, 8665.

(36) The binding selectivities of monosubstituted alkenes can also be compared to those of aldehydes. For example, the π/π' ratios for the propene and pentene complexes in Scheme 2 (**VI**/**VII**) are lower than those of the nearly isosteric acetaldehyde and butyraldehyde complexes **2h**,**j**$^+BF_4^-$ (Table 7). However, the styrene complex and benzaldehyde complex **1d**$^+BF_4^-$ exhibit an opposite trend. Regardless, these equilibria are measured at distinctly different temperatures and must be compared cautiously. It should also be noted that the rhenium−carbon bonds in the monosubstituted alkene complexes (Re−CHR, 2.23(1)−2.284(7) Å)[8a,b,g,9b] are longer than those in the aldehyde complexes (Charts 2 and 3).

Scheme 2. Binding Selectivities for Alkene Complexes of **I**[34]

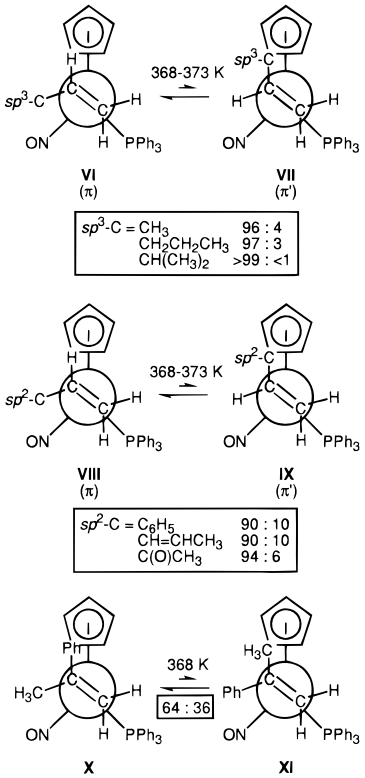

Scheme 3. Binding Selectivities for Other Aldehyde Complexes of **I**[34]

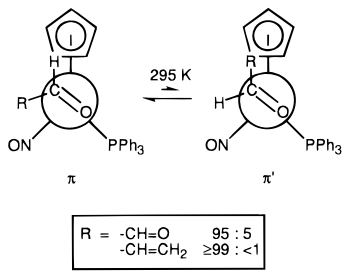

4. Although the energy differences involved are very small, these data indicate that chiral recognition can be influenced by species formally exogenous to the Lewis acid/base pair. Importantly, there is no evidence for any counteranion interactions in the above crystal structures.[37] The π/π' ratios appear to parallel the thermodynamic fluoride ion donor trend $BF_4^- > PF_6^- > SbF_6^-$.[38] Significant counteranion effects have previously been observed in the binding of chiral ammonium salts to chiral crown ethers.[1a]

Table 3 shows that concentration effects upon π/π' ratios are marked. The polarity of any medium becomes increasingly affected by the solute at higher concentrations. Also, $(\pi+\pi')/\sigma$ ratios *increase* in more polar solvents.[7d] However, π/π' ratios can only be assayed in a small number of solvents, all of which are chlorinated, due to a combination of freezing point limitations, insolubility (hydrocarbons, ethers), and reactivity (isopropyl alcohol). Aggregates would also be more likely to form at higher concentrations. However, racemic and enantiomerically pure **1d**$^+BF_4^-$ give identical π/π' ratios (Table 4). The structural and equilibrium properties of racemic and enantiomerically pure aggregates should differ markedly. Hence, we presently favor a polarity-based effect for the trends in Table 3.

When the crystal structures were manipulated on a stereoscopic screen, no other factors that should contribute to chiral recognition could be identified. The positions of the O═C hydrogen and aryl substituents were then interchanged, keeping carbon−hydrogen and carbon−carbon bond lengths and bend-back angles constant. When the resulting π' isomers were viewed with atoms set at van der Waals radii, the spatial overlaps of the aryl groups with the cyclopentadienyl ligands were modest. Thus, the interactions that give rise to the 1.2−0.4 kcal/mol energy differences in π/π' isomers are not visually striking. Importantly, crystal structures of the π and π' isomers of the styrene complex of **I** show virtually superimposable 11-atom (***C***$_5$)***Re***(***NO***)(***P***)(***C═C***) moieties.[8g] The rhenium−carbon bond lengths differ only slightly (Re−CHPh, 2.258(9) and 2.284(7) Å).

The preceding analysis suggests several modifications of the rhenium Lewis acid **I** that should enhance aldehyde or alkene enantioface binding selectivities. For example, the replacement of PPh_3 by a more electron-releasing but sterically equivalent phosphine such as P(*p*-tol)$_3$ would increase π basicity. This should strengthen backbonding, giving shorter rhenium−carbon bonds and higher π/π' ratios. Alternatively, a bulkier *pentamethyl*cyclopentadienyl ligand should enhance steric interactions with substituents in the π' isomers, raising π/π' ratios. This more electron-releasing ligand will also increase π basicity. Efforts to detect distinct π/π' isomers of pentamethylcyclopentadienyl aldehyde complexes $[(\eta^5\text{-}C_5Me_5)Re(NO)(PPh_3)(\eta^2\text{-}O{=}CHR)]^+BF_4^-$ by low temperature NMR have not yet been successful.[11a] However, the corresponding styrene and 1-pentene complexes exhibit much higher π/π' equilibrium ratios (>99:<1) than cyclopentadienyl analogs (Scheme 2).[11b]

3. Conclusion. The preceding data establish that a complex array of factors can influence chiral recognition in π complexes of chiral metal fragments and prochiral aldehydes or alkenes. Under standardized conditions with appropriately chosen compounds, marked electronic effects become apparent. In the cases of **1a**−**g**$^+X^-$, these are manifested in a key structural parameter—the distance between the rhenium and carbon stereocenters—the variation in which controls binding selectivities. This leads to the general prediction that chiral recognition will be enhanced when the π acidity of the ligand *or* the π basicity of the metal fragment is increased. To our knowledge, this represents a new approach to the optimization of chiral receptors, which are most commonly initially designed and then modified based upon steric principles.

With regard to metal-mediated enantioselective syntheses involving prochiral adlehydes and alkenes, it should be emphasized that the most stable isomer of an intermediate adduct need not be the most reactive.[39] For example, the σ isomer of **1a**$^+BF_4^-$ is much more reactive toward cyanide ion addition than the π/π' isomers.[7c] Nonetheless, even in these cases detailed bonding models must be developed to rationally optimize rates and stereoselectivities. In this context, a thorough study of the mechanism of interconversion of the π/π' isomers of **1a**−**g**$^+X^-$ is in progress and will be reported in due course.[16]

Experimental Section

General Methods. General procedures were given in a previous paper.[8c] Compounds were obtained or purified as follows: CH_2Cl_2 and C_6H_5Cl, distilled from P_2O_5; CD_2Cl_2, vacuum transferred from

(37) Distances between fluorine atoms of the anions and non-hydrogen atoms of the cations are all greater than 3.0 Å. Analogous distances to hydrogen atoms of the cations are greater than 2.3 Å.

(38) Honeychuck, R. V.; Hersh, W. H. *Inorg. Chem.* **1989**, *28*, 2869. However, this study shows that SbF_6^- forms stronger adducts than BF_4^- or PF_6^- with some Lewis acids.

(39) (a) Giovannetti, J. S.; Kelly, C. M.; Landis, C. R. *J. Am. Chem. Soc.* **1993**, *115*, 4040. (b) Bender, B. R.; Koller, M.; Nanz, D.; von Philipsborn, W. *J. Am. Chem. Soc.* **1993**, *115*, 5889. (c) Burk, M. J.; Feaster, J. E.; Nugent, W. A.; Harlow, R. L. *J. Am. Chem. Soc.* **1993**, *115*, 10125.

CaH_2; $CHCl_2F$, prepared by published methods;[22] ether, distilled from Na/benzophenone; aldehyde complexes not given below, prepared as reported earlier;[6a,c,7d] $HBF_4{\cdot}OEt_2$ (Aldrich), standardized before use;[40] $NH_4^+PF_6^-$, *p*-ethylbenzaldehyde (Aldrich), $Na^+SbF_6^-$ (AESAR), and other solvents, used as received.

[(η⁵-C_5H_5)Re(NO)(PPh₃)(O=CHC_6F_5)]⁺PF_6^- (1a⁺PF_6^-). A Schlenk flask was charged with **1a**$^+BF_4^-$ (0.037 g, 0.045 mmol),[7d] $NH_4^+PF_6^-$ (0.060 g, 0.37 mmol), and acetone (5 mL). The mixture was stirred for 10 min, and solvent was removed by oil pump vacuum. The residue was extracted with CH_2Cl_2 (5 mL). The extract was filtered through a medium porosity frit and concentrated to ca. 1 mL. Then ether (25 mL) was added with stirring. The yellow powder was collected by filtration and dried by oil pump vacuum to give **1a**$^+PF_6^-$ (0.035 g, 0.040 mmol, 89%), mp 184−189 °C dec.[41] Calcd for $C_{30}H_{21}F_{11}NO_2P_2Re$: C, 40.73; H, 2.39. Found: C, 40.69; H, 2.34. Yellow prisms were obtained from CH_2Cl_2/ether (−10 or 22 °C, vapor diffusion).

[(η⁵-C_5H_5)Re(NO)(PPh₃)(O=CH-4-C_6H_4Cl)]⁺PF_6^- (1c⁺PF_6^-). Complex **1c**$^+BF_4^-$ (0.039 g, 0.050 mmol),[7d] $NH_4^+PF_6^-$ (0.10 g, 0.61 mmol), and acetone (5 mL) were combined in a procedure analogous to that for **1a**$^+PF_6^-$. An identical workup gave **1c**$^+PF_6^-$ as a yellow powder (0.028 g, 0.034 mmol, 68%), mp 195−198 °C dec.[41] Calcd for $C_{30}H_{25}ClF_6NO_2P_2Re$: C, 43.46, H, 3.04. Found: C, 43.34; H, 3.02. Yellow prisms were obtained from CH_2Cl_2/ether (−10 °C, vapor diffusion).

[(η⁵-C_5H_5)Re(NO)(PPh₃)(O=CHC_6H_5)]⁺SbF_6^- (1d⁺SbF_6^-). Complex **1d**$^+BF_4^-$ (0.102 g, 0.135 mmol),[6a] $Na^+SbF_6^-$ (0.350 g, 1.35 mmol), and acetone (5 mL) were combined in a procedure analogous to that for **1a**$^+PF_6^-$. A similar workup (residue extracted with 25 mL of CH_2Cl_2) gave **1d**$^+SbF_6^-$ (0.082 g, 0.092 mmol, 68%), mp 186−188 °C dec.[41] Calcd for $C_{30}H_{26}F_6NO_2PReSb$: C, 40.69; H, 2.96. Found: C, 40.52; H, 3.01. Yellow prisms were obtained from CH_2Cl_2/ether (22 °C, vapor diffusion; 1:1 v/v methyl ethyl ketone/CH_2Cl_2 could also be substituted for CH_2Cl_2 (5 °C)).

[(η⁵-C_5H_5)Re(NO)(PPh₃)(O=CH-4-$C_6H_4CH_2CH_3$)]⁺X^- (1f⁺X^-). A. A Schlenk flask was charged with (η⁵-C_5H_5)Re(NO)(PPh_3)(CH_3) (0.374 g, 0.670 mmol)[42] and C_6H_5Cl (3 mL) and cooled to −45 °C. Then $HBF_4{\cdot}OEt_2$ (85 μL, 0.66 mmol) was added with stirring. After 20 min, *p*-ethylbenzaldehyde (0.245 g, 1.83 mmol) was added. After 25 min, the cold bath was removed. After 3 h, the mixture was added to ether (30 mL) with stirring. The red powder was collected by filtration, washed with ether (2 × 10 mL) and pentane (10 mL), and dried by oil pump vacuum to give **1f**$^+BF_4^-$ (0.446 g, 0.583 mmol, 87%), mp 107−110 °C dec.[43] Calcd for $C_{32}H_{30}BF_4NO_2PRe$: C, 50.27; H, 3.95. Found: C, 50.02; H, 4.15. **B.** Complex **1f**$^+BF_4^-$ (0.099 g, 0.13 mmol), $NH_4^+PF_6^-$ (0.215 g, 1.32 mmol), and acetone (5 mL) were combined in a procedure analogous to that for **1a**$^+PF_6^-$. An identical workup gave **1f**$^+PF_6^-$ (0.063 g, 0.076 mmol, 58%) as a red powder, mp 160−165 °C dec. Calcd for $C_{32}H_{30}F_6NO_2P_2Re$: C, 46.72; H, 3.68. Found: C, 46.60; H, 3.60. Bronze prisms were obtained from CH_2Cl_2/ether (5 °C, vapor diffusion in the presence of free *p*-ethylbenzaldehyde): IR (cm^{-1}, CH_2Cl_2/KBr) ν_{NO} 1735/1735 (π), 1701/1696 (σ); NMR (CD_2Cl_2) ^1H (δ) 7.66−7.44 (m, $3C_6H_5$), 7.39 (s, HCO), 7.26 (d, J_{HH} = 8.1 Hz, 2H of C_6H_4), 7.09 (d, J_{HH} = 8.1 Hz, 2H of C_6H_4), 5.78 (s, C_5H_5), 2.76 (q, J_{HH} = 7.5 Hz, CH_2), 1.23 (t, J_{HH} = 7.5 Hz, CH_3); $^{13}C\{^1H\}$ (ppm) PPh at 133.9 (d, J_{CP} = 10.3 Hz, *o*), 132.9 (d, J_{CP} = 2.8 Hz, *p*), 130.0 (d, J_{CP} = 11.2 Hz, *m*), 128.5 (d, J_{CP} = 58.6 Hz, *i*); CAr at 150.5 (s), 135.4 (s), 128.6 (s), 128.5 (s); 131.3 (s, CO), 97.7 (s, C_5H_5), 29.1 (s, CH_2), 15.5 (s, CH_3); $^{31}P\{^1H\}$ (ppm) 12.3 (s).

(40) Jablonski, C. R. *Aldrich. Acta* **1990**, *23*, 58.

(41) The ^1H NMR spectrum of IR ν_{NO} value were identical with those of the corresponding tetrafluoroborate salt.

(42) Agbossou, F.; O'Connor, E. J.; Garner, C. M.; Quirós Méndez, N.; Fernández, J. M.; Patton, A. T.; Ramsden, J. A.; Gladysz, J. A. *Inorg. Synth.* **1992**, *29*, 211.

(43) The IR (CH_2Cl_2) and ^1H and $^{31}P\{^1H\}$ NMR spectra were identical with those of **1f**$^+PF_6^-$.

Variable Temperature NMR. Data were acquired on Varian VXR-500 or XL-300 spectrometers as described earlier.[44] Probe temperatures were calibrated with methanol.[19] For the experiments in Tables 2−5 and 7, samples were prepared with freshly distilled solvent in volumetric flasks (tightly stoppered for $CHCl_2F$). Spectra were recorded after a 20 min equilibration period at each temperature. For the ^1H experiments in Table 7, samples were freeze−pump−thaw degassed three times. The optimum spinning and nonspinning shim values for a 1% solution of $CHCl_3$ in acetone-d_6 were determined using ShimIt (Dunkel, R. U.S. Patent No. 5,218,299). 500 MHz spectra were then recorded at 10 K intervals between 213 and 173 K. Uncorrectable magnet inhomogeneities gave multiple spinning side bands (ca. 1.4% of resonance height; Figure 1, bottom), so spectra of nonspinning samples were also recorded. The π/π′ ratios were determined gravimetrically from expanded spectra as described in the text.

Crystallography. Data were collected as summarized in Table 6.[25] Cell constants were obtained from 25−40 reflections ((*RS*,*SR*)-**1a**,**b**$^+PF_6^-$ (16 °C), (*RS*,*SR*)-**1d**$^+SbF_6^-$ (16 °C): 10° < 2θ < 20°; (*RS*,*SR*)-**1a**,**f**$^+PF_6^-$ (−80 °C), (*RS*,*SR*)-**1d**$^+SbF_6^-$ (−80 °C): 20° < 2θ < 30°; (*RS*,*SR*)-**1c**$^+PF_6^-$ (16 °C): 30° < 2θ < 40°; (*RS*,*SR*)-**1c**$^+PF_6^-$ (−125 °C): 16° < 2θ < 40°; (*RS*,*SR*)-**1f**$^+PF_6^-$ (16 °C): 28° < 2θ < 34°). Space groups were determined from systematic absences ((*RS*,*SR*)-**1a**,**f**$^+PF_6^-$, (*RS*,*SR*)-**1d**$^+SbF_6^-$: *h*0*l* *h* + *l* = 2*n*+1, 0*k*0 *k* = 2*n*+1; (*RS*,*SR*)-**1b**,**c**$^+PF_6^-$: none) and subsequent least-squares refinement. Lorentz, polarization, and empirical absorption (ψ scans) corrections were applied. The structures were solved by standard heavy-atom techniques with the SDP/VAX package.[45]

Hydrogen atoms were located as follows: (*RS*,*SR*)-**1a**,**c**$^+PF_6^-$ (−80, −125 °C) and (*RS*,*SR*)-**1b**$^+PF_6^-$ (16 °C), all; (*RS*,*SR*)-**1c**$^+PF_6^-$ (16 °C), O=CH-4-C_6H_4Cl; (*RS*,*SR*)-**1a**,**b**$^+PF_6^-$ (16 °C), (*RS*,*SR*)-**1f**$^+PF_6^-$ (16, −80 °C), O=CH; (*RS*,*SR*)-**1d**$^+SbF_6^-$ (16, −80 °C), none. Some were refined with fixed isotropic parameters: (*RS*,*SR*)-**1a**$^+PF_6^-$ (16 °C) and (*RS*,*SR*)-**1f**$^+PF_6^-$ (−80 °C), O=CH; (*RS*,*SR*)-**1a**$^+PF_6^-$ (−80 °C), all. The remaining hydrogen atom positions were calculated and added to the structure factor calculations but were not refined. The methyl group in (*RS*,*SR*)-**1f**$^+PF_6^-$ (C32) showed thermal and static disorder at 16 °C, and static disorder at −80 °C (ca. 70% occupancy). Scattering factors, and Δ*f*′ and Δ*f*″ values, were taken from the literature.[46]

Acknowledgment. We thank the NIH for support of this research.

Supporting Information Available: Table of NMR data for π/π′ isomers of **1**,**2**$^+X^-$ (individual runs), crystallographic data for (*RS*,*SR*)-**1a-c**,**f**$^+PF_6^-$ and (*RS*,*SR*)-**1d**$^+SbF_6^-$, views of the cations, and tables of atomic coordinates, bond lengths and angles, torsion angles, and anisotropic thermal parameters (28 pages). This material is contained in many libraries on microfiche, immediately follows this article in the microfilm version of the journal, can be ordered from the ACS, and can be downloaded from the Internet; see any current masthead page for ordering information and Internet access instructions. A color version of Figure 2 is available on the World Wide Web.

JA953523T

(44) (a) Buhro, W. E.; Zwick, B. D.; Georgiou, S.; Hutchinson, J. P.; Gladysz, J. A. *J. Am. Chem. Soc.* **1988**, *110*, 2427. (b) Zwick, B. D.; Dewey, M. A.; Knight, D. A.; Buhro, W. E.; Arif, A. M.; Gladysz, J. A. *Organometallics* **1992**, *11*, 2673.

(45) Frenz, B. A. In The Enraf-Nonius CAD 4 SDP—A Real-time System for Concurrent X-ray Data Collection and Crystal Structure Determination. In *Computing and Crystallography*; Schenk, H., Olthof-Hazelkamp, R., van Konigsveld, H., Bassi, G. C., Eds.; Delft University Press: Delft, Holland, 1978; pp 64−71.

(46) Cromer, D. T.; Waber, J. T. In *International Tables for X-ray Crystallography*; Ibers, J. A., Hamilton, W. C., Eds.; Kynoch: Birmingham, England, 1974; Volume IV, pp 72−98, 149−150; tables 2.2B and 2.3.1.